The long-chain fatty acid-CoA ligase FadD1 monitors *Pseudomonas aeruginosa* quorum sensing as a receptor of *cis*-2-decenoic acid

Shihao Song[1,2,11], Xia Li[3,11], Jingyun Liu[2,4,11], Bing Wang[1], Yang Si[5], Hongguang Han[1], Xiuyun Sun[1,3], Mingfang Wang[3], Binbin Cui[3,6], Guangliang Wu[6], Yongliang Huo[7], Liangxiong Xu[8], Beile Gao[9], Liang Yang[10], Xiaoxue Wang[9], Lian-Hui Zhang[2], Yinyue Deng[3,*]

[1]*Key Laboratory of Tropical Biological Resources of Ministry of Education, School of Pharmaceutical Sciences, Hainan University, Haikou 570228, China*

[2]*Integrative Microbiology Research Center, South China Agricultural University, Guangzhou 510642, China*

[3]*School of Pharmaceutical Sciences (Shenzhen), Shenzhen Campus of Sun Yat-sen University, Sun Yat-sen University, Shenzhen 518107, China*

[4]*Zhengzhou Shuqing Medical College, Zhengzhou 450064, China*

[5]*Department of Microbiology, College of Life Sciences, Nanjing Agricultural University, Nanjing 210095, China*

[6]*Pharmacy Department, The Affiliated LiHuiLi Hospital of Ningbo University, Ningbo315046, China*

[7]*Experimental Animal Center, Guangzhou Medical University, Guangzhou, Guangdong, 511436, China*

[8]*School of Life Sciences, Huizhou University, Huizhou 516007, China*

[9]*Guangdong Key Laboratory of Marine Materia Medica, South China Sea Institute of Oceanology, Chinese Academy of Sciences, Guangzhou 510301, China*

[10]*School of Medicine, Southern University of Science and Technology, Shenzhen 518055, China.*

[11]*These authors contributed equally: Shihao Song, Xia Li and Jingyun Liu.*

Corresponding author:

Yinyue Deng: dengyle@mail.sysu.edu.cn

Running title: *Cis*-2-decenoic acid controls *P. aeruginosa* virulence

Abstract

Diffusible signal factor (DSF)-family quorum sensing (QS) signals are widely utilized by many bacterial pathogens to modulate various biological functions and virulence. Previous studies showed that *cis*-2-decenoic acid (*cis*-DA) is involved in modulation of biofilm dispersion in *Pseudomonas aeruginosa*, but its signaling mechanism remains vague. Here, we report that *cis*-DA regulates the physiology and virulence of *P. aeruginosa* through the long-chain fatty acid-CoA ligase FadD1. *Cis*-DA specifically binds to FadD1 with high affinity and enhances the binding of FadD1 to the promoter DNA region of *lasR*. Further analysis showed that the FadD1 is a response regulator of *cis*-DA with a DNA-binding leucine zipper motif to control the transcription of various target genes. Moreover, FadD1 exhibited catalytic activity on *cis*-2-dodecenoic acid (BDSF) of *Burkholderia cenocepacia* and enhanced the competitiveness of *P. aeruginosa*. Together, our work presents a new DSF-type QS signaling system, which is highlighted by its receptor and response regulator evolved from a canonical enzyme of fatty acid metabolism.

Introduction

Quorum sensing (QS) is a cell-to-cell communication mechanism utilized by numerous species of bacteria. The first QS signal discovered in gram-negative bacteria is the acyl homoserine lactone (AHL) produced by *Vibrio fischeri*[1-5]. In addition to AHL-family signals, there are many other types of QS signals[6-16], including the diffusible signal factor (DSF)-family signals. *Pseudomonas aeruginosa* is a major source of opportunistic infections in both immunocompromised individuals and cystic fibrosis patients and has evolved at least three types of QS systems, e.g., *las*, *pqs* and *rhl*[17-19]. The *las* and *rhl* AHL QS systems use N-3-oxo-dodecanoyl-l-homoserine lactone (3-oxo-C12-HSL) and N-butyryl-l-homoserine lactone (C4-HSL), respectively, to regulate biological functions, such as biofilm formation, motility and virulence factor production[20-24]. The *pqs* system employs 2-heptyl-3-hydroxy-4(1H)-quinolone (PQS), to regulate biological functions and virulence[25-29]. These QS systems of *P. aeruginosa* are hierarchically interrelated, and the *las* system was verified to monitor both the *rhl* and *pqs* systems[17, 30]. Moreover, it was also revealed that the fatty acid signaling molecule *cis*-2-decenoic acid (*cis*-DA) exhibited important functions in *P. aeruginosa*[31]. The production of *cis*-DA in *P. aeruginosa* needs an enoyl-CoA synthase encoded by DspI[32]. The inactivation of DspI leads to a significant reduction in biofilm dispersion[33,34]. However, it is not yet clear how *cis*-DA regulates biofilm

dispersion, and its receptor and downstream signaling network remain to be investigated.

Fatty acyl coenzyme A (CoA) synthetases (FACSs; fatty acid-CoA ligases) are a class of enzymes that activate alkanoic acids to CoA esters[35]. FACSs are widely distributed in both prokaryotic and eukaryotic organisms and exhibit broad substrate specificity[36]. The long-chain fatty acid-CoA ligase (FadD) is responsible for the activation of endogenous long-chain fatty acids into acyl-CoAs[37]. RpfB, which has recently been reported as a long-chain fatty acid-CoA ligase of *Xanthomonas campestris* pv. campestris (*Xcc*), is involved in the activation of a wide range of fatty acids to their CoA esters *in vitro*[38]. Intriguingly, RpfB is required for the turnover of both *cis*-11-methyl-dodecenoic acid (DSF) and *cis*-2-dodecenoic acid (BDSF) QS signals *in vivo*[39]. The *rpfB* deletion mutant produced high levels of both DSF and BDSF signals and displayed increased virulence in *Xcc*[40,41]. Moreover, RpfB-dependent QS signal turnover was also detected in various bacterial species[40].

Transcription factors (TFs) are proteins that bind to specific DNA sequences, thereby regulating the transcription of genetic information from DNA to messenger RNA[42]. Once bound to DNA, these proteins can promote or block the recruitment of RNA polymerase to specific genes to control transcriptional expression[43]. Although there is great diversity in the structure and function of DNA-binding proteins, some polypeptide motifs enable binding to the major groove of DNA, including helix-turn-helix (HTH), helix-loop-helix (HLH), zinc fingers, and leucine zippers[44-47].

In this study, we demonstrated that FadD1 of *P. aeruginosa* could convert BDSF to *cis*-2-dodecenoic acid-CoA and reduce the competitiveness of *B. cenocepacia*. FadD1 also controls the physiology and virulence of *P. aeruginosa* by sensing *cis*-DA, then monitors the QS hierarchy and controls the expression of various target genes as a global transcriptional regulator. These findings indicate that FadD1 is a member of a new class of response regulators of QS signal that controls the important biological functions and virulence of bacterial pathogens, with an additional role in fatty acid oxidation to catalyze the formation of fatty acyl-CoA.

Results

FadD1 of *P. aeruginosa* shows enzyme activity on the BDSF signal

BDSF was first found to be involved in the regulation of biofilm formation, motility and virulence of *B. cenocepacia*[9-12,48,49]. It was subsequently reported that BDSF from *B. cenocepacia* interferes with QS systems and the type III secretion system (T3SS) of *P. aeruginosa*[50]. Interestingly, we found that

90 BDSF could also be degraded when it was added to the culture of *P. aeruginosa* PAO1. The amount
91 of BDSF in the culture of *P. aeruginosa* decreased to 21.78% after 6 h of incubation (Fig. 1a). Previous
92 work demonstrated that RpfB is a long-chain fatty acid-CoA ligase responsible for BDSF and DSF
93 signal turnover in *Xcc*[38,39]. To discover the enzyme that degrades BDSF, we then searched RpfB
94 homologs in the genome of *P. aeruginosa* PAO1 by using the Basic Local Alignment Search Tool
95 (BLAST) algorithm[51]. We found six RpfB homologs, FadD1-6[52]; among them, FadD1 showed the
96 highest homology, with 55.35% identity with RpfB. Therefore, FadD1, which contains 562 aa with a
97 calculated molecular weight of 61.67 kDa, was purified to homogeneity using affinity chromatography
98 (Fig. 1b). The *in vitro* enzymatic activity assays showed that when FadD1 was mixed with BDSF, the
99 free BDSF level in the mixture decreased nearly undetectable after 1 h (Fig. 1c). These results
100 suggested that FadD1 exhibits enzyme activity on BDSF. Consistently, deletion of *fadD1* in *P.*
101 *aeruginosa* caused a substantial reduction in BDSF degradation activity (Fig. 1d) but did not affect
102 the growth rate of the bacterial cells (Supplementary Fig. 1).
103 We then investigated the *in vivo* activity of FadD1 in *B. cenocepacia* H111 by overexpressing the
104 *fadD1* gene. Overexpression of *fadD1* did not affect the growth rate but markedly reduced the BDSF
105 production of the bacterial cells (Supplementary Fig. 2a, b). As expected, deletion of $rpfF_{Bc}$ resulted
106 in complete abolishment of the production of BDSF in *B. cenocepacia* H111 (Supplementary Fig. 2b).
107 Interestingly, overexpression of *fadD1* in the *B. cenocepacia* wild-type strain reduced biofilm formation,
108 swarming motility and protease activity, which could be restored by the addition of exogenous BDSF
109 at 5 μM (Supplementary Fig. 2c-e). Overexpression of *fadD1* in the wild-type strain H111 also
110 decreased cytotoxicity (Supplementary Fig. 2f).
111
112 **FadD1 boosts the competitive capability of *P. aeruginosa* against *B. cenocepacia***
113 As BDSF mediates the cross-talk between *B. cenocepacia* and *P. aeruginosa* [50] and FadD1 exhibits
114 catalysis activity on BDSF, we investigated whether FadD1 plays a role in the competitive interactions
115 between the two bacterial species. To this end, we cocultured the green fluorescent protein (GFP)
116 fluorescence-labeled *P. aeruginosa* PAO1 wild-type, Δ*fadD1* and complemented strains in the
117 presence of the *B. cenocepacia* H111 strain labeled with mCherry and measured the BDSF production
118 of *B. cenocepacia* (Fig. 1d) and the mean fluorescence intensity (MFI) of both *B. cenocepacia* and *P.*
119 *aeruginosa* at different time points as indicated (Fig. 1e, f). The results showed that deletion of *fadD1*

caused a drastic reduction in the degradation capability of *P. aeruginosa* toward the BDSF signal. The BDSF signal yield of *B. cenocepacia* cocultured with the *P. aeruginosa* deletion mutant Δ*fadD1* was more than 5 times higher than that when it was cocultured with wild-type PAO1 or the complemented strain Δ*fadD1*(*fadD1*) at 9 h postinoculation (Fig. 1d). On the other hand, we found that the GFP mean fluorescence intensity (MFI) of the *P. aeruginosa* Δ*fadD1* strain was lower than that of the *P. aeruginosa* wild-type and complemented strains when they were cocultured with the *B. cenocepacia* strains (Fig. 1e). The mCherry mean fluorescence intensity (MFI) of the *B. cenocepacia* H111 strain cocultured with the *P. aeruginosa* Δ*fadD1* strain was higher than that of the *B. cenocepacia* H111 strain cocultured with the *P. aeruginosa* wild-type and complemented strains (Fig. 1f). These results indicated that FadD1 plays an important role in the competition between *P. aeruginosa* and *B. cenocepacia*.

Deletion of FadD1 impairs biological functions and pathogenicity in *P. aeruginosa*

It was determined that FadD1 plays an important role in the interaction between *P. aeruginosa* and *B. cenocepacia*. We continued to study whether FadD1plays a role in the regulation of biological functions and pathogenesis in *P. aeruginosa*. We found that deletion of *fadD1* resulted in decreases in biofilm formation, swarming, and pyocyanin production by 30.47%, 36.72% and 62.15%, respectively (Fig. 2a-c). Deletion of *fadD1* also attenuated cytotoxicity by 69.78% when A549 cells were incubated with the *P. aeruginosa* strains at 8 h postinoculation (Fig. 2d). We tested whether there was a change in the expression level of upstream (*PA3298*) and downstream (*fadD2*) genes of the *fadD1* mutant gene. The results showed that there was no change in the expression of upstream and downstream genes in the *fadD1* deletion mutant (Supplementary Fig. 3). To further study the regulatory roles of FadD1 in controlling bacterial physiology, we analyzed and compared the transcriptomes of the wild-type strain and the Δ*fadD1* mutant strain by using RNA sequencing (RNA-Seq). Differential gene expression analysis showed that the expression levels of 23 genes were increased and those of 208 genes were decreased in the Δ*fadD1* mutant strain compared with the expression levels in the wild-type strain (|Log_2 fold-change| ≥ 1.0) (Supplementary Table 1 and Supplementary Fig. 4a). These differentially expressed genes are associated with a range of biological functions (Supplementary Table 1 and Supplementary Fig. 4b). These genes include the *las*, *rhl* and *pqs* QS system genes *PA1432* (*lasI*), *PA1430* (*lasR*), *PA3476* (*rhlI*), *PA3477* (*rhlR*),

PA0996 (*pqsA*), and *PA1003* (*mvfR*), which were shown to be involved in pathogenicity in *P. aeruginosa*.

FadD1 monitors the QS systems of *P. aeruginosa*

As FadD1 obviously affects the QS-regulated genes and phenotypes of *P. aeruginosa* (Fig. 2a-d, Supplementary Fig. 4 and Supplementary Table 1), we inferred that FadD1 might affect the QS systems. Analysis of the expression profiles of *lacZ* under the control of the *lasR*, *lasI*, *rhlR*, *rhlI*, *mvfR* and *pqsA* promoters showed that deletion of *fadD1* resulted in reduced expression levels of *lasR*, *lasI*, *rhlR*, *rhlI*, *mvfR* and *pqsA* (Fig. 2e-j), which are signal molecule receptor genes and synthase-encoding genes of the *las*, *rhl* and *pqs* QS systems, respectively. RT-qPCR analysis and RNA-seq also showed that the mutation of *fadD1* caused a decrease in the expression levels of *lasR*, *lasI*, *rhlR*, *rhlI*, *mvfR* and *pqsA* (Fig. 2k). Therefore, we measured and compared the production of 3-oxo-C12-HSL, C4-HSL and PQS in the wild-type, *fadD1* mutant, and complemented strains. We found that the production of 3-oxo-C12-HSL, C4-HSL and PQS was reduced in the *fadD1* mutant strain (Fig. 2l-n). These results demonstrated that FadD1 positively regulated the *las*, *rhl* and *pqs* QS systems in *P. aeruginosa*.

FadD1 regulates target gene expression by directly binding to the promoter

FadD1 obviously affects the QS gene expression levels and QS signal production of *P. aeruginosa*. Therefore, we performed electrophoretic mobility shift assays (EMSAs) to test whether the transcriptional regulation of the signal molecule synthase-encoding genes and receptor genes of the *las*, *rhl* and *pqs* QS systems is achieved by direct binding of FadD1 to their promoters. The 339-bp, 321-bp, 270-bp, 330-bp, 306-bp and 324-bp DNA fragments from the *lasR*, *lasI*, *rhlR*, *rhlI*, *mvfR* and *pqsA* promoters were PCR-amplified and used as probes. Surprisingly, as shown in Figure. 3*A*, the *lasR* promoter DNA fragment formed stable DNA-protein complexes with FadD1 and migrated slower than unbound probes. The amount of labeled probe that bound to FadD1 increased with increasing amounts of FadD1 but decreased in the presence of a 50-fold greater concentration of unlabeled probe (Fig. 3a). However, FadD1 did not bind to the promoters of the other tested genes, i.e., *rhlR*, *mvfR*, *lasI*, *rhlI* and *pqsA* (Supplementary Fig. 5 and 6).

To identify the DNA motif recognized by FadD1 and the genes directly regulated by FadD1, we

performed chromatin immunoprecipitation sequencing (ChIP-Seq) analysis. ChIP-Seq data analysis revealed the potential FadD1 binding site as 5'-AGGACGG-3' in the *lasR* gene promoter probe (Fig. 3b). The results showed that FadD1 could directly bind to multiple target gene promoters to regulate their transcription and expression (Supplementary Table 2). To further examine the binding sites, three target genes, *flgM*, *katA* and *PA0692,* were chosen for EMSA analysis. The amounts of labeled probes of *flgM*, *katA* and *PA0692* bound to FadD1 were also increased with increasing amounts of FadD1 (Supplementary Fig. 7). Then, the potential binding sites 5'-AGGACGG-3', 5'-TGGCCGG-3', 5'-AGGAGGG-3', and 5'-AGGGCGG-3' were deleted from the promoter regions of *lasR*, *flgM*, *katA* and *PA0692*, respectively. EMSA analysis showed that no DNA-protein complex was formed when the binding site was deleted from the probes (Fig. 3c and Supplementary Fig. 8), indicating that this fragment is essential for the binding of FadD1 to the *lasR, flgM*, *katA* and *PA0692* promoters. Together, these results demonstrated that FadD1 regulates target gene expression by directly binding to a specific region in the gene promoter.

The leucine zipper motif of FadD1 is responsible for binding with DNA

Since FadD1 can bind to *lasR* and regulate transcription, and the domain structure analysis of FadD1 by using the HMMER (https://www.ebi.ac.uk/Tools/hmmer/) shows that it has an AMP-binding enzyme domain (AMP-B) and an AMP-binding enzyme C-terminal domain (AMP-B_C) (Fig. 3d). We then purified the AMP-B domain and the AMP-B_C domain for EMSA (Fig. 3e). The results showed that only the AMP-B domain can bind to the promoter region of *lasR* (Fig. 3f, g). To determine the location of the new DNA binding motif in the AMP-B domain, we used the protein motif analysis website (https://www.novopro.cn/tools/motifscan.html). A structure called "leucine zipper" was characterized at 275 to 296 amino acids **L**TGNHNI**L**ITNPRD**L**PSMLKD**L** in AMP-B domain (Fig. 3d and Supplementary Fig. 9). The leucine zipper consists of a periodic repetition of leucine residues at every seventh position over a distance covering eight helical turns. This motif is found in many eukaryotic transcription factors[45]. However, in bacterial transcription factor, this motif is only found in the classical DNA-binding HTH domain of the LysR family regulator MetR[46] and a BDSF response regulator DsfR identified recently[47]. So we speculated that the four leucine residues L275, L282, L289 and L296 might be important for the binding of FadD1 to target gene promoters. We then introduced four site-specific substitutions into FadD1 (named FadD1^{LM}), and the results showed that the simultaneous

210 mutation of L275A, L282A, L289A and L296A abolished the binding of FadD1 to the *lasR* promoter
211 (Fig. 3i). In addition, *in trans* expression of FadD1^{LM} did not rescue the defective biofilm, swarming
212 motility and pyocyanin production phenotypes of the Δ*fadD1* strain (Fig. 3j-l). We then used the
213 HDOCK server to automatically predict the interaction between FadD1 and the DNA-binding site 5'-
214 AGGACGG-3'. The binding model of DNA and FadD1 and the detailed contacts of the complex are
215 shown in Supplementary Fig. 10 and Supplementary Table 3, respectively. The binding sites of FadD1
216 are in the leucine zipper structure. The results are consistent with the conclusion that the DNA-binding
217 motif of FadD1 is the leucine zipper.
218
219 **FadD1 is a receptor of *cis*-DA**
220 Since *cis*-DA is a DSF-type QS signal in *P. aeruginosa*, and the FadD1 controls QS-regulated
221 phenotypes as a global transcriptional regulator in *P. aeruginosa*, we then measured whether there is
222 an interaction between *cis*-DA and FadD1. To test this hypothesis, we purified FadD1 to performed
223 microscale thermophoresis (MST) analysis to test whether FadD1 binds *cis*-DA. As shown in Fig. 4a,
224 FadD1 exhibited binding activity to *cis*-DA, with an estimated dissociation constant (K_D) of 1.06 ± 0.14
225 μM. To further confirm FadD1 is a receptor of *cis*-DA, we generated the *cis*-DA deficient mutant Δ*dspI*,
226 the double deletion mutants Δ*dspI*Δ*fadD1* and *in trans* expressed *fadD1* in the Δ*dspI* and measured
227 the motility activity and pyocyanin of these strains. The results showed that *in trans* expression of
228 *fadD1* rescued the defective motility and pyocyanin phenotypes of the Δ*dspI* strain (Fig. 4b, c).
229 Interestingly, we found that the addition of exogenous *cis*-DA rescued the impaired motility and
230 pyocyanin of Δ*dspI* (Fig. 4b, c); however, addition of exogenous *cis*-DA showed no effect on these
231 phenotypes of the mutant Δ*fadD1* and Δ*dspI*Δ*fadD1* (Fig. 4b, c). We then measured the gene
232 expression levels of *lasR*, *lasI*, *rhlR*, *rhlI*, *mvfR* and *pqsA* in the wild-type strain and the Δ*dspI* strain.
233 The results indicated that deletion of *dspI* caused a significant decrease in the gene expression levels
234 of *las*, *rhl* and *pqs* QS system genes (Fig. 4d-i). Therefore, we measured and compared the production
235 of 3-oxo-C12-HSL, C4-HSL and PQS in the wild-type, *dspI* mutant, and complemented strains. The
236 result showed that the production of 3-oxo-C12-HSL, C4-HSL and PQS was reduced in the *dspI*
237 mutant strain (Fig. 4j-l). These results demonstrated that both *cis*-DA and FadD1 positively regulates
238 the *las*, *rhl* and *pqs* QS systems in *P. aeruginosa*.
239

240 ***cis*-DA enhances the binding of FadD1 to target gene promoters**

241 To determine how the binding of *cis*-DA to FadD1 might affect the activity of FadD1, we examined the
242 effects of *cis*-DA on the binding of FadD1 to the *lasR* promoter by EMSA. As shown in Fig. 5a, the
243 binding of FadD1 to the promoter probe of *lasR* was enhanced when *cis*-DA was present in the
244 reaction mixtures, and the amount of probe bound to FadD1 increased as the amount of *cis*-DA
245 increased (Fig. 5a).

246 Then, we attempted to identify the *cis*-DA-binding sites in FadD1. Autodocking analysis revealed 2
247 amino acid residues, Gly488 (G488) and Arg552 (R552), that might be critical for the interaction
248 between FadD1and *cis*-DA (Fig. 5b). To test whether the roles of these acid residues are related to
249 the binding to *cis*-DA, we then generated two single point mutants (FadD1^{G488A} and FadD1^{R552A}) (Fig.
250 5c). MST analysis showed that the mutant FadD1^{G488A} and FadD1^{R552A} did not bind to *cis*-DA (Fig. 5d,
251 e). Consistent with this, EMSA analysis showed that mutation of the *cis*-DA-binding site (Gly488 and
252 Arg552) completely eliminated the effect of *cis*-DA on FadD1 (Fig. 5f, g). In addition, *in trans*
253 expression of *fadD1*^{G488A} and *fadD1*^{R552A} only partially rescued motility and pyocyanin (Fig. 5h, i), and
254 the addition of exogenous 20 μM *cis*-DA showed no effect on these phenotypes of the mutant
255 Δ*dspI*Δ*fadD1*(*fadD1*^{G488A}) and Δ*dspI*Δ*fadD1*(*fadD1*^{R552A}) (Fig. 5h, i). Thus, we concluded that FadD1
256 is a specific response regulator of *cis*-DA in *P. aeruginosa*.

257

258 **Reconstruction of FadD2 with the leucine zipper motif**

259 Our study found that the DNA binding motif of FadD1 is a leucine zipper motif. Therefore, we used
260 the protein motif analysis website (https://www.novopro.cn/tools/motifscan.html) to analyze whether
261 the other FadD proteins, FadD2-6, contain a leucine zipper structure. The results showed that the
262 other FadD proteins did not contain a leucine zipper structure, and EMSA analysis showed that FadD2,
263 which shares about 59.82% amino acid identity with FadD1, did not bind to the *lasR* gene promoter
264 (Supplementary Fig. 11a, b). To further investigate the role of the leucine zipper motif of FadD1, we
265 reconstructed FadD2 by adding the leucine zipper structure of FadD1 to the same part of FadD2
266 (named FadD2$_{LZ}$) and tested whether the reconstructed FadD2 has regulatory activity similar to that
267 of FadD1. Therefore, FadD2$_{LZ}$ was purified to homogeneity using affinity chromatography
268 (Supplementary Fig. 11c), and assayed whether it could bind to the *lasR* promoter. Intriguingly, we
269 found that the *lasR* promoter DNA fragment formed stable DNA-protein complexes with FadD2$_{LZ}$ and

migrated more slowly than unbound probes. The amount of labeled probe that bound to $FadD2_{LZ}$ increased with increasing amounts of $FadD2_{LZ}$ but decreased in the presence of a 50-fold greater concentration of unlabeled probe (Supplementary Fig. 11d). Interestingly, addition of exogenous *cis*-DA also enhanced the binding of $FadD2_{LZ}$ to the *lasR* promoter probe at a final concentration of 20 μM (Supplementary Fig. 11e). In addition, *in trans* expression of the *fadD2*$_{LZ}$ gene rescued the defective swarming motility and pyocyanin production phenotypes of the Δ*fadD1* strain (Supplementary Fig. 11f, g). And we also found that the addition of exogenous *cis*-DA rescued the impaired motility and pyocyanin of Δ*dspI*Δ*fadD1*(*fadD2*$_{LZ}$) (Supplementary Fig. 11f, g). These results showed that the leucine zipper motif plays a critical role in the regulatory activity of FadD1.

Analysis of the catalytic motif of FadD1

Previous studies reported that fatty acyl-CoA ligase plays a crucial role in catalyzing the formation of fatty acyl-CoA through hydrolysis of pyrophosphate[35,36]. To test whether FadD1 can function in the uptake and activation steps of fatty acid degradation, we evaluated its enzymatic activity *in vitro*. The results showed that FadD1 had high activity on lauric acid (C12:0), while it displayed moderate activity on BDSF but no activity on *cis*-DA (Supplementary Fig. 12a). In addition, the previous study found that mutation of Trp433, Thr436 and Arg453, the substrate binding sties, results in complete inactivation of fatty acyl-CoA synthetase in *E. coli* (37). We continued to generated three single point mutants ($FadD1^{W434A}$, $FadD1^{T437A}$ and $FadD1^{R454A}$) to explore whether the mutation affects the enzyme activity of FadD1 (Supplementary Fig. 12b). Similarly, it was shown that the $FadD1^{W434A}$, $FadD1^{T437A}$ and $FadD1^{R454A}$ exerted no enzyme activity on *cis*-DA, BDSF and lauric acid (C12:0) (Supplementary Fig. 12c-e). To further characterize the relationship between enzyme activity of FadD1 and perception of *cis*-DA, we chose to test the regulatory activity of the mutant $FadD1^{R454A}$. We *in trans* expressed the *fadD1*^{R454A} in the Δ*dspI*Δ*fadD1* mutant strain. Interestingly, it was found that addition of exogenous *cis*-DA rescued the impaired motility of Δ*dspI*Δ*fadD1*(*fadD1*^{R454A}) (Supplementary Fig. 12f). Consistent with this, EMSA analysis showed that mutation of the substrate binding stie (Arg454) would not affect the perception of *cis*-DA (Supplementary Fig. 12g).

Homologs of FadD1 are widespread in bacteria

To determine whether FadD1 is widely distributed, homologs of FadD1 were sought in the genome

database by using the BLAST program. It was indicated that homologs of FadD1 are distributed across many different bacterial species, including in the genera *Pseudomonas*, *Azotobacter*, *Azomonas*, and *Halopseudomonas* (Supplementary Table 4). Furthermore, the homologs of FadD1 in the genera *Pseudomonas, Azotobacter* and *Azomonas* contain a leucine zipper structure (Supplementary Table 4). We then selected *P. fluorescens* Migula ATCC17518, which contains both a $FadD1_{Pf}$ protein with a leucine zipper structure and a $lasR_{Pf}$ gene, and the $FadD1_{Pf}$ protein was purified by affinity chromatography and tested for its interaction with the $lasR_{Pf}$ gene promoter. The EMSA results showed that the $FadD1_{Pf}$ protein from *P. fluorescens* could also bind to the $lasR_{Pf}$ gene promoter (Supplementary Fig. 13), indicating that the transcriptional regulatory mechanism of FadD1 might be widely conserved in bacteria.

Discussion

Fatty acid-CoA ligase plays a vital role in fatty acid metabolism, as it can convert fatty acids to fatty acyl-CoA in bacteria[37]. In this study, we found that the fatty acid-CoA ligase FadD1 of *P. aeruginosa* not only exhibits high activity for the catalysis of lauric acid (C12:0) to lauric acid-CoA (Supplementary Figure. 12a), and employs a key role in the bacterial competition with *B. cenocepacia* by degrading its QS signal BDSF (Fig. 1), but also plays a critical role in the regulation of *P. aeruginosa* physiology and pathogenesis by acting as the receptor and response regulator of its QS signal *cis*-DA (Fig. 2 and Supplementary Table 1). We demonstrated that FadD1 can directly bind to the promoter of the target genes, thereby regulate the transcription levels of the target genes (Fig. 3a and Supplementary Fig. 7). It was further identified that mutation of the leucine zipper structure of FadD1 abolished the binding of FadD1 to the target gene promoters (Fig. 3i). Interestingly, we found that FadD2 does not contain a leucine zipper structure, and EMSA analysis showed that FadD2 did not bind to the *lasR* gene promoter (Supplementary Fig. 11b). However, the reconstructed FadD2 with addition of the leucine zipper structure of FadD1 to the same part of FadD2 (named $FadD2_{LZ}$) obtained the regulatory activity similar to that of FadD1. It could bind to the *lasR* gene promoter and restore the *fadD1* mutant phenotypes (Supplementary Fig. 11). Furthermore, our findings indicate that FadD1 is widely conserved in many other bacterial species, including *Pseudomonas*, *Azotobacter*, and *Azomonas* species (Supplementary Table 4), indicating that FadD1 with a leucine zipper structure might be a new family of transcriptional regulatory proteins widely conserved in bacteria.

330 The fatty acid molecule *cis*-DA was first identified in *P. aeruginosa* to act as the autoinducer of
331 biofilm dispersion[31]. It has also been shown to induce biofilm dispersion in a range of Gram-negative
332 and Gram-positive bacteria and in the fungal pathogen *Candida albicans*[31]. Although the previous
333 study reported that the two-component sensor/response regulator hybrid DspS (PA4112, PA14_10770)
334 is required and essential for native biofilm dispersion in response to the cell-to-cell signaling molecule
335 *cis*-DA[34], there was no exploration of other functions of *cis*-DA. In this study, we found that deletion of
336 *dspI*, which is the synthase of *cis*-DA, caused an impairment in motility and pyocyanin production (Fig.
337 4b, c). Interestingly, in *trans* expression of *fadD1* rescued the defective motility and pyocyanin
338 phenotypes of the Δ*dspI* strain (Fig. 4b, c). However, the addition of exogenous *cis*-DA showed no
339 effect on these phenotypes of the mutant Δ*fadD1* and Δ*dspI*Δ*fadD1* (Fig. 4b, c). Moreover, *cis*-DA is
340 shown to bind to FadD1 with high affinity and enhanced the binding of FadD1 to the target gene
341 promoter probes (Fig. 4a, 5a). We also identified that two amino acid residues at positions Gly488
342 (G488) and Arg552 (R552) are critical for the interaction between FadD1 and *cis*-DA (Fig. 5).
343 Mutations at Gly488 and Arg552 abolished the binding between FadD1 and *cis*-DA (Fig. 5d, e).
344 Another interesting observation in this study was that mutation at the substrate binding stie Arg454
345 (R454) completely abolished the enzyme activity of FadD1 on both BDSF and lauric acid (C12:0)
346 (Supplementary Fig. 12c-e), but could not affect the effect of *cis*-DA on FadD1 (Supplementary Fig.
347 12g), suggesting that the *cis*-DA-binding site is different from the substrate-binding stie in FadD1.
348 Together, FadD1 was identified to be a new response regulator of *cis*-DA QS signal.
349 BDSF has been identified to be a DSF-family QS signal in *B. cenocepacia*[11]. As *cis*-DA shares a
350 similar chemical structure with that of BDSF, we then continued to explore the interaction between
351 BDSF and FadD1. Although FadD1 showed a degradation activity on BDSF, we found that FadD1
352 tightly binds to BDSF with an estimated dissociation constant (K_D) of 1.65 ± 0.21 μM (Supplementary
353 Fig. 14a). Interestingly, the addition of exogenous BDSF also enhanced the binding of FadD1 to the
354 *lasR* promoter probe at a final concentration of 10 μM (Supplementary Fig. 14b). To distinguish the
355 role of BDSF to be a “substrate” or “ligand” of FadD1, we then used EMSA analysis and the result
356 showed that mutation of the *cis*-DA-binding sites abolished the perception of *cis*-DA (Fig. 5), but will
357 not affect the effect of BDSF on FadD1 (Supplementary Fig. 14c). However, EMSA analysis showed
358 that mutation of the substrate-binding stie (Arg454) completely abolished the effect of BDSF on the
359 binding of FadD1 to target gene promoter (Supplementary Fig. 14d), while not affect the effect of *cis*-

DA on FadD1 (Supplementary Fig. 12g). These results suggested that BDSF also interferes with the binding of FadD1 to target gene promoters *in vitro* as a substrate of the canonical enzyme FadD1.

In *P. aeruginosa,* there are at least three QS systems, namely, *las*, *rhl* and *pqs*, which are involved in the regulation of a broad range of genes important for metabolism and virulence[18,19]. These QS systems are hierarchically interrelated, and the *las* system was verified to monitor both the *rhl* and *pqs* systems[17,30]. In this study, we identified that FadD1 affects the QS-regulated phenotypes, including the biofilm formation, swarming, and pyocyanin in *P. aeruginosa* (Fig. 2a-c). Surprisingly, we also identified that FadD1 is a *cis*-DA receptor protein that positively regulates the *las*, *rhl* and *pqs* QS systems in *P. aeruginosa* (Fig. 2, 6). These results indicated that FadD1 is not only a response regulator of *cis*-DA but also an important upstream regulator of the QS signaling network in *P. aeruginosa*. FadD1 regulates numerous target genes and physiological functions by monitoring the QS signaling systems, which broadens our understanding of the QS signaling network of *P. aeruginosa*.

In summary, our findings suggest that FadD1, which contains a leucine zipper structure in the AMP-B domain, is not only an enzyme of fatty oxidation but also a receptor of *cis*-DA that directly controls target gene expression and controls the QS network in *P. aeruginosa*. In addition, the BLAST search revealed that homologs of FadD1 containing the leucine zipper structure are highly conserved in many bacteria (Supplementary Table 4), suggesting that the regulatory mechanism of FadD1 might be present in various bacterial species. Consistently, our recent study revealed that the fatty acyl-CoA ligase DsfR (BCAM2136), which contains a leucine zipper motif, acts as a global transcriptional regulator to control *B. cenocepacia* virulence by sensing BDSF[47]. Different from FadD1, DsfR has a specific BDSF-sensing site and showed no enzyme activity on BDSF, while FadD1 only binds with BDSF on the substrate-binding sites. These results indicate that FadD1 and DsfR share some common characteristics and are distinguished from each other. In conclusion, our work presents a unique and widely conserved signal receptor of *cis*-DA, which might be an important new type of QS signal receptor in bacteria.

Methods

Bacterial strains and growth conditions.

The bacterial strains and plasmids used in this work are listed in Supplementary Table 5. *P. aeruginosa*

390 PAO1, *P. fluorescens* Migula ATCC17518 and *B. cenocepacia* H111 strains obtained from the
391 American Type Culture Collection (ATCC) were maintained in Luria-Bertani broth (LB; 10 g/L tryptone,
392 5 g/L yeast extract (#PL0021, oxoid), 5 g/L NaCl (#S805275, Macklin)) at 37°C. The following
393 antibiotics were added when necessary: ampicillin (#A830931, Macklin) and kanamycin (#K885955,
394 Macklin) at 100 μg mL^{-1}; tetracycline (#T829835, Macklin), 10 μg mL^{-1}; and gentamicin (#G810322,
395 Macklin), 10 μg mL^{-1}. BDSF (#C957977, Macklin) and *cis*-DA (#Z911073, Macklin) (HPLC ≥ 99%)
396 were dissolved in methanol at a final concentration of 100 mM, and this solution was added to the
397 medium in the experiments. Bacterial growth was determined by measuring the optical density at 600
398 nm.
399
400 **BSDF extraction**
401 The extraction of BDSF from culture supernatants was conducted following previously described
402 methods[11,53]. To quantify BDSF production in the culture of *B. cenocepacia* strain or *P. aeruginosa*
403 strain, 100 mL of the supernatant was collected. Its crude ethyl acetate (#E809178, Macklin) extract
404 was passed through a 0.22 μm Minisart filter unit (#16541-K, Sartorius) and was then condensed to
405 1 mL for LC-MS analysis.
406
407 **Quantification of BDSF and *cis*-DA**
408 Quantification of BDSF and *cis*-DA was performed by using an LC-MS system, which consisted of an
409 ACQUITY UPLC system and a Waters Q-Tof Premier high-resolution mass spectrometer[53]. An
410 ACQUITY UPLC BEH C18 column 1.7 μm (2.1 × 50 mm) was used for the chromatography analysis
411 of BDSF and *cis*-DA, which was eluted with a CH_3OH (methyl alcohol, #A452, ThermoFisher) gradient
412 in water at 65-100% supplemented with 0.01% formic acid at a flow rate of 0.4 $mL \cdot min^{-1}$ for 10 min.
413 Next, 65% CH_3OH was used for 3 min. The entire elution column was introduced into the Q-TOF mass
414 spectrometer according to the manufacturer's instructions. The BDSF and *cis*-DA levels in the culture
415 supernatant were measured using the peak area in the extracted ion chromatogram.
416
417 **Protein expression and purification**
418 The coding regions of proteins were amplified with the primers listed in Supplementary Table 6, and
419 were attached and fused to the expression vectors pET-21a, pET-28a and PDBHT2. The fusion gene

420 constructs were transformed into *E. coli* strain BL21. Affinity purification of the 6×His fusion proteins
421 was performed using Ni-NTA resin (#SA035010, Smart-lifesciences). The His-tag was removed using
422 TEV protease (#P2307, Beyotime), and the cleaved fusion protein was analyzed by SDS-PAGE[54,55].
423

424 **Enzyme activity assays**

425 The activity of FadD1 was determined following the methods[56]. *cis*-DA, BDSF or lauric acid (C12:0)
426 were dissolved in TME buffer (Tris-HCl (#T917657, Macklin), 60 mM; $MgCl_2$ (#M813763, Macklin), 10
427 mM; EDTA (#E885215, Macklin), 1 mM; coenzyme A (CoASH) (#C824132, Macklin), 0.5 mM; and
428 Triton X-100 (#T6328, Macklin), 0.1%; pH 7.5) and added to the mixture at a final concentration of
429 200 μM, while the final concentrations of FadD1 and its derivatives were 20 μM. The reaction mixture
430 was incubated at 37°C, and the reaction was stopped by placing sample tubes in boiling water for 5,
431 15, 30 and 60 min. *cis*-DA, BDSF or lauric acid (C12:0) levels were measured by LC-MS spectrometry.
432

433 **Construction of in-frame deletion mutants and complementation**

434 *P. aeruginosa* PAO1 was used as the parental strain for the generation of an in-frame deletion mutant
435 of *fadD1* and *dspI* by the following method described previously[14]. The primers used to generate
436 upstream and downstream regions flanking *fadD1* and *dspI* are listed in Supplementary Table 7. For
437 complementation analysis, the coding regions of *fadD1* and *dspI* were amplified by PCR and cloned
438 into the plasmid pBBR1-MCS5, pBBR1-MCS2 and pLAFR3 using the primers listed in Supplementary
439 Table 6. The resulting constructs were conjugated into the *P. aeruginosa* PAO1 mutant, *B.*
440 *cenocepacia* H111 strain by electroporation[14,54].
441

442 **Bacterial growth analysis**

443 An overnight bacterial culture in LB medium was inoculated into fresh media to an OD_{600} of 0.01. A
444 10 mL cell suspension was grown in 50 mL conical centrifuge tubes at 37°C with shaking at 220 rpm.
445 Bacterial growth was determined by measuring the optical density at 600 nm every 4 hours. LB
446 medium was used as the negative control[47].
447

448 **Competition assays in the mixed culture**

449 The green fluorescent protein expression vector was used and transformed into the *P. aeruginosa*

450 PAO1 WT, Δ*fadD1* and Δ*fadD1*(*fadD1*) strains. The mCherry fluorescent protein expression vector
451 was introduced into the *B. cenocepacia* H111 strain by electroporation. Then, the *P. aeruginosa* PAO1
452 WT, Δ*fadD1* and Δ*fadD1*(*fadD1*) strains were cocultured with the *B. cenocepacia* H111 strain at an
453 initial ratio of 1:4 (vol/vol) at OD_{600} = 0.1 at 37°C with shaking at 220 rpm for 12 h. Then, the
454 quantification of BDSF was performed by using an LC-MS system, and the mixed cultures were
455 analyzed by a Spectra Max i3x multifunctional enzyme labeling instrument (Molecular Devices, CA,
456 USA)[57].
457
458 ***P. aeruginosa* phenotype assays**
459 For the analysis of biofilm formation[58], bacterial cells were grown overnight at 37°C and inoculated
460 into LB media (150 μL per well) in 96-well polypropylene microtiter plates. Microtiter plates with fitted
461 lids were incubated at 37°C with shaking at 200 rpm for 12 h. The plates were then washed to remove
462 planktonic cells and stained for 20 min with 1% (weight/vol) crystal violet (#C6158, Sigma-Aldrich).
463 After washing with water, 200 μL of 95% (vol/vol) ethanol was added to the wells to release the stain.
464 Biofilm was determined by measuring the absorbance of the resulting solution at 570 nm.
465 Motility was determined on 0.3% semisolid agar (#BD214010, Becton, Dickinson and Company).
466 Bacteria were inoculated into the center of plates containing 0.8% tryptone, 0.5% glucose, and 0.3%
467 agar. The plates were incubated at 30°C for 18 h before the diameter of the colony was measured[54].
468 The pyocyanin assay was performed with the method described previously[49]. Briefly, bacteria were
469 cultured at 37°C for approximately 12 hours and centrifuged at 13,000 rpm for 1 min, and 1.5 mL
470 supernatants were collected and extracted with double volume chloroform with vigorous shaking at
471 room temperature for 30 min. The solvent phase was transferred to a new tube containing 1 mL of 1
472 N HCl (#H399545, Sigma-Aldrich). The mixture was shaken gently to transfer pyocyanin to the
473 aqueous phase. The quantity of pyocyanin was determined by measurement of absorbance at 520
474 nm and normalization against the cell density.
475
476 ***B. cenocepacia* phenotype assays**
477 Biofilm formation in 96-well polypropylene microtiter dishes was assayed essentially as described
478 previously by *P. aeruginosa*. Swarming motility was determined on semisolid agar (0.3%). Bacteria
479 were inoculated into the center of plates containing 0.8% tryptone, 0.5% glucose, and 0.3% agar. The

480 plates were incubated at 30°C for 18 h before the diameter of the colony was measured.

481 Protease assays were performed following a previously described method[14]. Briefly, bacteria were
482 cultured at 37°C for approximately 12 hours. Cultures were centrifuged at 13,000 rpm for 5 min, and
483 the supernatants were removed and filtered through a 0.22 μm membrane. One hundred microliters
484 of supernatant was incubated at 30°C with an equal volume of azocasein (#A875599, Macklin)
485 dissolved in proteolytic buffer (5 mg/mL) for 30 min. The reaction was stopped by the addition of 400
486 μL of 10% (weight/vol) TCA (#T818877, Macklin) buffer. After incubation for 2 min at room temperature,
487 the mixture was centrifuged at 13,000 rpm for 1 min to remove the remaining azocasein. Supernatants
488 were removed and mixed with 700 μL of 525 mM NaOH (#S817977, Macklin). The absorbance of the
489 azopeptide supernatant was measured at a wavelength of 442 nm. Protease activity was obtained
490 after normalization of the absorbance against the corresponding cell density.

491

492 **Cytotoxicity assays**

493 Cytotoxicity was assessed by measuring the release of LDH from human A549 cells[54]. The A549 cell
494 line was cultured in Dulbecco's modified Eagle's medium (#D6429, Sigma-Aldrich) at 37°C with 5%
495 CO_2. A549 cells were seeded in 96-well plates at a density of 5×10^4 cells per well and grown until
496 they reached ~90% confluence. Culture supernatants were removed, and the cell monolayer was
497 washed once with phosphate-buffered saline (PBS). Fresh bacterial cells cultured to an OD_{600} of 1.0
498 were washed and diluted in DMEM. The diluted bacterial cells were then added to the A549 cell
499 monolayers at a multiplicity of infection (MOI) of approximately 1000. After incubation for 8 h, the
500 cytotoxicity was determined by measuring the released lactate dehydrogenase (LDH) in the
501 supernatants using a cytotoxicity detection kit (#4744926001, Roche).

502

503 **Construction of reporter strains and measurement of β-galactosidase activity**

504 The promoters of *lasR, lasI, rhlR*, *rhlI, mvfR* and *pqsA* were amplified using the primer pairs listed in
505 Supplementary Table 6. The resulting products were inserted upstream of the promoter less *lacZ* gene
506 in the vector pME2-*lacZ*. Transconjugants were then selected on LB agar plates supplemented with
507 tetracycline and X-gal (#X8050, Solarbio). Measurement of β-galactosidase activities was performed
508 following previously described methods[14,54,55].

509

510 **Quantitative reverse transcription PCR assays**

511 Bacterial cells were cultured at 37°C in LB broth to the logarithmic-growth phase (OD_{600}=1.0). Cells
512 were collected by centrifugation, and total RNA was extracted using an Eastep Super Total RNA
513 Extraction Kit (#LS1040, Promega). cDNA synthesis was performed using a HiScript III 1st Strand
514 cDNA Synthesis Kit (#11141ES60, Yeasen). Primers for RT-qPCR are listed in Supplementary Table
515 6. The RT-qPCR experiments were performed on a QuantStudio™ 7 RT-qPCR System (Thermo
516 Fisher) using SYBR qPCR Green Master Mix (#11201ES08, Yeasen). The expression of the target
517 genes was normalized to the expression level of 16S RNA. The relative transcript abundance was
518 calculated by the $2^{-\Delta\Delta Ct}$ method[55]. At least three biological replicates were performed per sample.

519

520 **Quantitative analysis of QS signal production in *P. aeruginosa***

521 Bacterial cells were grown in LB medium overnight with agitation at 37°C. One liter of culture
522 supernatant was collected by centrifugation and extracted with an equal volume of ethyl acetate. The
523 crude extract (organic phase) was dried using a rotary evaporator and dissolved in methanol. All of
524 the above samples were kept at 4°C until analysis. Ultrahigh-performance liquid chromatography-
525 electrospray ionization tandem mass spectrometry (UHPLC-ESI-MS/MS) was performed in a
526 Shimadzu LC-30A UHPLC system with a Waters C18 column (1.8 μm, 150 × 2.1 mm) and a Shimadzu
527 8060 QQQ-MS mass spectrometer with an ESI source interface. The mass spectrometer was
528 operated in positive-ion mode. The mobile phase was prepared as 0.1% formic acid/water and
529 acetonitrile[57].

530

531 **RNA-Seq analysis**

532 RNA was isolated from *P. aeruginosa* strains grown to OD_{600}=1.0 by using the Eastep Super Total
533 RNA Extraction Kit (Promega, Madison, USA). The concentration was measured using a Qubit® RNA
534 Assay Kit in a Qubit® 2.0 Fluorometer (Life Technologies, CA, USA). The purity and integrity were
535 checked using the NanoPhotometer® spectrophotometer (IMPLEN, CA, USA) and the RNA Nano
536 6000 Assay Kit of the Bioanalyzer 2100 system (Agilent Technologies, CA, USA), respectively.
537 Sequencing libraries were generated using the NEBNext® Ultra™ Directional RNA Library Prep Kit
538 for Illumina® (NEB, USA) and then purified by the AMPure XP system. Finally, library quality was
539 assessed by using the Agilent Bioanalyzer 2100 system. The clustering of the index-coded samples

was performed on a cBot Cluster Generation System using TruSeq PE Cluster Kit v3-cBot-HS (Illumina). After cluster generation, the library preparations were sequenced on an Illumina HiSeq platform, and paired-end reads were generated. Trimmed sequence reads were aligned to the *P. aeruginosa* PAO1 genome sequence using Bowtie2-2.2.3, and normalized read counts were compared using HTSeq v0.6.1 as described previously[59,60]. Then, the FPKM of each gene was calculated based on the 26 lengths of this gene, and the read count was mapped to the gene.

Electrophoretic gel mobility shift assay

Electrophoretic mobility shift assay (EMSA) experiments were performed as described previously[53,54,61]. The DNA probes used for EMSA were prepared by PCR amplification using the primer pairs listed in Supplementary Table 6. The purified PCR products were 3-end-labeled with biotin following the manufacturer's instructions (#20148, Thermo Fisher). The DNA-protein binding reactions were performed according to the manufacturer's instructions (#20148, Thermo Fisher). A 5% polyacrylamide gel was used to separate the DNA-protein complexes. After UV cross-linking, the biotin-labeled probes were detected in the membrane using a Biotin luminescent detection kit (#20148, Thermo Fisher).

Chromatin immunoprecipitation sequencing analyses

Chromatin immunoprecipitation sequencing (ChIP-Seq) was performed according to previously published methods with some modifications[62]. ChIP-Seq analysis was conducted by the Wuhan IGENEBOOK Biotechnology Co. Ltd. (Wuhan, China). The anti-HIS antibody (ab9108, 1:1000, Abcam) was used for immunoprecipitation, and DNA fragments enriched by ChIP were sequenced on an Illumina HiSeq 2000. After removing sequencing adaptors and low-quality bases, the clean reads were mapped to the *P. aeruginosa* PAO1 genome using BWA software (version 0.7.15-r1140). The peak caller MACS (version, 2.1.1.20160309; *q* value, 0.05) was used to localize the potential binding sites of FadD1[63].

Molecular docking FadD1

The 3D structure of the double-stranded DNA was built in the MOE1 DNA/RNA Builder. Protein-DNA docking in the HDOCK2 server was used for molecular docking simulation of FadD1 and DNA[64,65].

570 The 3D structure of FadD1 (Q9HYU4) predicted by AlphaFold2 was set as the receptor, and the 3D
571 structure of the DNA was set as the ligand[66]. The HDOCK server automatically predicts their
572 interaction through a hybrid algorithm of template-based and template-free docking. First, the server
573 performs template-based modeling to identify possible homologous DNA templates. Second, the
574 intrinsic scoring function for protein-RNA interactions is integrated in template-free docking. Finally,
575 the top 100 predicted complex structures are provided to users for download, of which the top 10
576 models will be visualized on the result web page. The intermolecular contacts from the most likely
577 poses were further evaluated. The models of the complex and interface residues were analyzed using
578 MOE. Molecular graphics were generated by PyMOL.

579 AutoDock and PyMOL were used for docking and binding site analysis. The crystal structure of
580 FadD1 from the AlphaFold2 was used for docking with *cis*-DA by AutoDock software. To screen the
581 potential binding sites, a grid box was prepared to wrap the entire macromolecule. The receptor grid
582 was centered at center_x = -1.038, center_y = 1.49, center_z = 11.31, size_x = 126, size_y = 126, and
583 size_z = 126. The exhaustiveness was set at 50. The top scoring ligand conformation was chosen,
584 and the potential binding sites were visualized in 3D by PyMOL. The potential binding sites were
585 visualized in 2D by Protein Plus (https://proteins.plus/).

586

587 **Microscale thermophoresis assay**

588 Protein-binding experiments were carried out with a Nano Temper 16 Monolith NT.115 instrument
589 (NanoTemper Technologies; www.nanotemper-technologies.com)[55]. In brief, the protein was labeled
590 with the L014 Monolith NT.115 Protein Labelling Kit (#MO-L018, Nano Temper). The labeled protein
591 and different titers of unlabeled *cis*-DA were mixed and loaded onto standard treated silicon capillaries
592 (#MO-L022, Nano Temper), and fluorescence was measured. The measurements were carried out at
593 20% LED power and 40% MST power.

594

595 **Statistical analysis**

596 No statistical method was used to predetermine the sample size. No data were excluded from the
597 analyses. The data are presented as the means ± standard deviations. Statistical analyses were
598 performed with Prism 8 software (GraphPad). Statistical significance is indicated as follows: $^{*}p < 0.05$;
599 $^{**}p < 0.01$; $^{***}p < 0.001$; ns = no significance (one-way ANOVA or two-way ANOVA). Biological

replicates and numbers of independent experiments were stated in the legends. All experiments presented as representative LC-MS graphs or gels were repeated at least 3 times with similar results.

Reporting summary

Further information on the research design is available in the Nature Research Reporting Summary linked to this article.

Data Availability

RNA-seq and ChIP-seq data generated in this study have been deposited in the National Center for Biotechnology Information Sequence Read Archive (SRA) database under accession code PRJNA1121197 (https://www.ncbi.nlm.nih.gov/bioproject/PRJNA1121197) and PRJNA1120965 (https://www.ncbi.nlm.nih.gov/bioproject/PRJNA1120965), respectively. The data supporting the findings of this study are available within the article and Supplementary Information file.

Reference

1. Nealson, K.H. & Hastings, J.W. Bacterial bioluminescence: its control and ecological significance. *Microbiol. Rev.* **43**, 496-518 (1979). doi: 10.1128/mr.43.4.496-518.1979.
2. Fuqua, C. & Greenberg, E.P. Listening in on bacteria: acyl-homoserine lactone signalling. *Nat. Rev. Mol. Cell Biol.* 3, 685-695 (2002). doi: 10.1038/nrm907.
3. Papenfort, K. & Bassler, B.L. Quorum sensing signal-response systems in Gram-negative bacteria. *Nat. Rev. Microbiol.* **14**, 576-588 (2016). doi: 10.1038/nrmicro.2016.89.
4. Whiteley, M., Diggle, S.P. & Greenberg, E.P. Progress in and promise of bacterial quorum sensing research. *Nature* **551**, 313-320 (2017). doi: 10.1038/nature24624.
5. Chadha, J., Harjai, K. & Chhibber, S. Revisiting the virulence hallmarks of *Pseudomonas aeruginosa*: a chronicle through the perspective of quorum sensing. *Environ. Microbiol.* **24**, 2630-2656 (2022). doi: 10.1111/1462-2920.15784.
6. Flavier, A.B., Clough, S.J., Schell, M.A. & Denny, T.P. Identification of 3-hydroxypalmitic acid methyl ester as a novel autoregulator controlling virulence in *Ralstonia solanacearum*. *Mol. Microbiol.* **26**, 251-259 (1997). doi: 10.1046/j.1365-2958.1997.5661945.x.
7. Barber, C.E. *et al.*, A novel regulatory system required for pathogenicity of *Xanthomonas campestris* is mediated by a small diffusible signal molecule. *Mol. Microbiol.* **24**, 555-566 (1997). doi: 10.1046/j.1365-2958.1997.3721736.x.
8. Déziel, E. *et al.*, Analysis of *Pseudomonas aeruginosa* 4-hydroxy-2-alkylquinolines (HAQs) reveals a role for 4-hydroxy-2-heptylquinoline in cell-to-cell communication. *Proc. Natl Acad. Sci. U.S.A.* **101**, 1339-1344 (2004). doi: 10.1073/pnas.0307694100.
9. Zhang, L.H. & Dong, Y.H. Quorum sensing and signal interference: diverse implications. *Mol. Microbiol.* **53**, 1563-1571 (2004). doi: 10.1111/j.1365-2958.2004.04234.x.

10. Diggle, S.P. *et al.*, The *Pseudomonas aeruginosa* 4-quinolone signal molecules HHQ and PQS play multifunctional roles in quorum sensing and iron entrapment. *Chem. Biol.* **14**, 87-96 (2007). doi: 10.1016/j.chembiol.2006.11.014.
11. Boon, C. *et al.*, A novel DSF-like signal from *Burkholderia cenocepacia* interferes with *Candida albicans* morphological transition. *ISME J.* **2**, 27-36 (2008). doi: 10.1038/ismej.2007.76.
12. He, Y.W. & Zhang, L.H. Quorum sensing and virulence regulation in *Xanthomonas campestris*. *FEMS Microbiol. Rev.* **32**, 842-57 (2008). doi: 10.1111/j.1574-6976.2008.00120.x.
13. Deng, Y., Wu, J., Tao, F. & Zhang, L.H. Listening to a new language: DSF-based quorum sensing in Gram-negative bacteria. *Chem. Rev.* **111**, 160-173 (2011). doi: 10.1021/cr100354f.
14. Deng, Y. *et al.*, *Cis*-2-dodecenoic acid receptor RpfR links quorum-sensing signal perception with regulation of virulence through cyclic dimeric guanosine monophosphate turnover. *Proc. Natl Acad. Sci. U.S.A.* **109**, 15479-15484 (2012). doi: 10.1073/pnas.1205037109.
15. Dulcey, C.E. *et al.*, The end of an old hypothesis: the *pseudomonas* signaling molecules 4-hydroxy-2-alkylquinolines derive from fatty acids, not 3-ketofatty acids. *Chem. Biol.* **20**, 1481-1491 (2013). doi: 10.1016/j.chembiol.2013.09.021.
16. Wang, M., Li, X., Song, S., Cui, C., Zhang, L.H. & Deng, Y. The *cis*-2-Dodecenoic Acid (BDSF) Quorum Sensing System in *Burkholderia cenocepacia*. *Appl. Environ. Microbiol.* **88**, e0234221 (2022). doi: 10.1128/aem.02342-21.
17. de Kievit, T.R., Kakai, Y., Register, J.K., Pesci, E.C. & Iglewski, B.H. Role of the *Pseudomonas aeruginosa las* and *rhl* quorum-sensing systems in *rhlI* regulation. *FEMS Microbiol. Lett.* **212**, 101-106 (2002). doi: 10.1016/s0378-1097(02)00735-8.
18. Lee, J. & Zhang, L.H. The hierarchy quorum sensing network in *Pseudomonas aeruginosa*. *Protein Cell* **6**, 26-41 (2015). doi: 10.1007/s13238-014-0100-x.
19. Mukherjee, S., Moustafa, D., Smith, C.D., Goldberg, J.B. & Bassler, B.L. The RhlR quorum-sensing receptor controls *Pseudomonas aeruginosa* pathogenesis and biofilm development independently of its canonical homoserine lactone autoinducer. *PLoS Pathog.* **13**, e1006504 (2017). doi: 10.1371/journal.ppat.1006504.
20. Fuqua, W.C., Winans, S.C. & Greenberg, E.P. Quorum sensing in bacteria: the LuxR-LuxI family of cell density-responsive transcriptional regulators. *J. Bacteriol.* **176**, 269-275 (1994). doi: 10.1128/jb.176.2.269-275.1994.
21. Pesci, E.C., Pearson, J.P., Seed, P.C. & Iglewski, B.H. Regulation of *las* and *rhl* quorum sensing in *Pseudomonas aeruginosa*. *J. Bacteriol.* **179**, 3127-3132 (1997). doi: 10.1128/jb.179.10.3127-3132.
22. Withers, H., Swift, S. & Williams, P. Quorum sensing as an integral component of gene regulatory networks in Gram-negative bacteria. *Curr. Opin. Microbiol.* **4**, 186-193 (2001). doi: 10.1016/s1369-5274(00)00187-9.
23. Ng, W.L. & Bassler, B.L. Bacterial quorum-sensing network architectures. *Annu. Rev. Genet.* **43**, 197-222 (2009). doi: 10.1146/annurev-genet-102108-134304.
24. Rutherford, S.T. & Bassler, B.L. Bacterial quorum sensing: its role in virulence and possibilities for its control. *C.S.H. Perspect. Med.* **2**, a012427 (2012). doi: 10.1101/cshperspect.a012427.
25. Jander, G., Rahme, L.G. & Ausubel, F.M. Positive correlation between virulence of *Pseudomonas aeruginosa* mutants in mice and insects. *J. Bacteriol.* **182**, 3843-3845 (2000). doi: 10.1128/JB.182.13.3843-3845.
26. Cao, H., Krishnan, G., Goumnerov, B., Tsongalis, J., Tompkins, R. & Rahme, L.G. A quorum

681 sensing-associated virulence gene of *Pseudomonas aeruginosa* encodes a LysR-like
682 transcription regulator with a unique self-regulatory mechanism. *Proc. Natl Acad. Sci. U.S.A.* **98**,
683 14613-14618 (2001). doi: 10.1073/pnas.251465298.
684 27. Wade, D.S. *et al.*, Regulation of *Pseudomonas* quinolone signal synthesis in *Pseudomonas*
685 *aeruginosa*. *J. Bacteriol.* **187**, 4372-4380 (2005). doi: 10.1128/JB.187.13.4372-4380.
686 28. Déziel, E. *et al.*, The contribution of MvfR to *Pseudomonas aeruginosa* pathogenesis and quorum
687 sensing circuitry regulation: multiple quorum sensing-regulated genes are modulated without
688 affecting *lasRI*, *rhlRI* or the production of N-acyl-L-homoserine lactones. *Mol. Microbiol.* **55**, 998-
689 1014 (2005). doi: 10.1111/j.1365-2958.2004.04448.x.
690 29. García-Reyes, S., Soberón-Chávez, G. & Cocotl-Yanez, M. The third quorum-sensing system of
691 *Pseudomonas aeruginosa*: *Pseudomonas* quinolone signal and the enigmatic PqsE protein. *J.*
692 *Med. Microbiol.* **69**, 25-34 (2020). doi: 10.1099/jmm.0.001116.
693 30. Choi, Y. *et al.*, Growth phase-differential quorum sensing regulation of anthranilate metabolism in
694 *Pseudomonas aeruginosa*. *Mol. Cells* **32**, 57-65 (2011). doi: 10.1007/s10059-011-2322-6.
695 31. Davies, D.G. & Marques, C.N. A fatty acid messenger is responsible for inducing dispersion in
696 microbial biofilms. *J. Bacteriol.* **191**, 1393-1403 (2009). doi: 10.1128/JB.01214-08.
697 32. Amari, D.T., Marques, C.N. & Davies, D.G. The putative enoyl-coenzyme A hydratase DspI is
698 required for production of the *Pseudomonas aeruginosa* biofilm dispersion autoinducer *cis*-2-
699 decenoic acid. *J. Bacteriol.* **195**, 4600-4610 (2013). doi: 10.1128/JB.00707-13.
700 33. Rahmani-Badi, A., Sepehr, S., Fallahi, H. & Heidari-Keshel, S. Dissection of the *cis*-2-decenoic
701 acid signaling network in *Pseudomonas aeruginosa* using microarray technique. *Front. Microbiol.*
702 **6**, 383 (2015). doi: 10.3389/fmicb.2015.00383.
703 34. Kalia, M., Amari, D., Davies, D.G. & Sauer, K. *cis*-DA-dependent dispersion by *Pseudomonas*
704 *aeruginosa* biofilm and identification of *cis*-DA-sensory protein DspS. *mBio*. **14**, e0257023 (2023).
705 doi: 10.1128/mbio.02570-23.
706 35. Hume, A.R., Nikodinovic-Runic, J. & O'Connor, K.E. FadD from *Pseudomonas putida* CA-3 is a
707 true long-chain fatty acyl coenzyme A synthetase that activates phenylalkanoic and alkanoic acids.
708 *J. Bacteriol.* **191**, 7554-7565 (2009). doi: 10.1128/JB.01016-09.
709 36. Ruth, K., de Roo, G., Egli, T. & Ren, Q. Identification of two acyl-CoA synthetases from
710 *Pseudomonas putida* GPo1: one is located at the surface of polyhydroxyalkanoates granules.
711 *Biomacromolecules* **9**, 1652-1659 (2008). doi: 10.1021/bm8001655.
712 37. Black, P.N., Zhang, Q., Weimar, J.D. & DiRusso, C.C. Mutational analysis of a fatty acyl-coenzyme
713 A synthetase signature motif identifies seven amino acid residues that modulate fatty acid
714 substrate specificity. *J. Biol. Chem.* **272**, 4896-4903 (1997). doi: 10.1074/jbc.272.8.4896.
715 38. Bi, H., Yu, Y., Dong, H., Wang, H. & Cronan, J.E. *Xanthomonas campestris* RpfB is a fatty Acyl-
716 CoA ligase required to counteract the thioesterase activity of the RpfF diffusible signal factor (DSF)
717 synthase. *Mol. Microbiol.* **93**, 262-275 (2014). doi: 10.1111/mmi.12657.
718 39. Zhou, L., Wang, X.Y., Sun, S., Yang, L.C., Jiang, B.L. & He, Y.W. Identification and characterization
719 of naturally occurring DSF-family quorum sensing signal turnover system in the phytopathogen
720 *Xanthomonas*. *Environ. Microbiol.* **17**, 4646-4658 (2015). doi: 10.1111/1462-2920.12999.
721 40. Wang, X.Y., Zhou, L., Yang, J., Ji, G.H. & He, Y.W. The RpfB-Dependent Quorum Sensing Signal
722 Turnover System Is Required for Adaptation and Virulence in Rice Bacterial Blight Pathogen
723 *Xanthomonas oryzae* pv. oryzae. *Mol. Plant Microbe. Interact.* **29**, 220-230 (2016). doi:
724 10.1094/MPMI-09-15-0206-R.

41. Tian, X.Q., Wu, Y., Cai, Z. & Qian, W. BDSF is a degradation-prone quorum-sensing signal detected by the histidine kinase RpfC of *Xanthomonas campestris* pv. *campestris*. *Appl. Environ. Microbiol.* **88**, e0003122 (2022). doi: 10.1128/aem.00031-22.
42. Maston, G.A., Evans, S.K. & Green, M.R. Transcriptional regulatory elements in the human genome. *Annu. Rev. Genomics. Hum. Genet.* **7**, 29-59 (2006). doi: 10.1146/annurev.genom.7.080505.115623.
43. Wang, G., Wang, F., Huang, Q., Li, Y., Liu, Y. & Wang, Y. Understanding Transcription Factor Regulation by Integrating Gene Expression and DNase I Hypersensitive Sites. *Biomed. Res. Int.* **2015**, 757530 (2015). doi: 10.1155/2015/757530.
44. Clark, D.P. & Pazdernik, N.J. Chapter e14 - Protein Structure and Function, *Mol. Biol. (Second Edition)*, 2013, Pages e280-e284, https://doi.org/10.1016/B978-0-12-378594-7.00048-2.
45. Miller, M. The importance of being flexible: the case of basic region leucine zipper transcriptional regulators. *Curr. Protein Pept. Sci.* **10**, 244-269 (2009). doi: 10.2174/138920309788452164.
46. Maxon, M.E., Wigboldus, J., Brot, N. & Weissbach, H. Structure-function studies on *Escherichia coli* MetR protein, a putative prokaryotic leucine zipper protein. *Proc. Natl Acad. Sci. U.S.A.* **87**, 7076-7079 (1990). doi: 10.1073/pnas.87.18.7076.
47. Li, X. *et al.*, Regulation of *Burkholderia cenocepacia* virulence by the fatty acyl-CoA ligase DsfR as a response regulator of quorum sensing signal. *Cell Rep.* **43**, 114223 (2024). doi: 10.1016/j.celrep.2024.114223.
48. Deng, Y., Boon, C., Eberl, L. & Zhang, L.H. Differential modulation of *Burkholderia cenocepacia* virulence and energy metabolism by the quorum-sensing signal BDSF and its synthase. *J. Bacteriol.* **191**, 7270-7278 (2009). doi: 10.1128/JB.00681-09.
49. Deng, Y., Wu, J., Eberl, L. & Zhang, L.H. Structural and functional characterization of diffusible signal factor family quorum-sensing signals produced by members of the *Burkholderia cepacia* complex. *Appl. Environ. Microbiol.* **76**, 4675-4683 (2010). doi: 10.1128/AEM.00480-10.
50. Deng, Y., Boon, C., Chen, S., Lim, A. & Zhang, L.H. *Cis*-2-dodecenoic acid signal modulates virulence of *Pseudomonas aeruginosa* through interference with quorum sensing systems and T3SS. *BMC Microbiol.* **13**, 231 (2013). doi: 10.1186/1471-2180-13-231.
51. Altschul, S.F., Gish, W., Miller, W., Myers, E.W. & Lipman, D.J. Basic local alignment search tool. *J. Mol. Biol.* **215**, 403-410 (1990). doi: 10.1016/S0022-2836(05)80360-2.
52. Zarzycki-Siek, J. *et al.*, Elucidating the *Pseudomonas aeruginosa* fatty acid degradation pathway: identification of additional fatty acyl-CoA synthetase homologues. *PLoS One* **8**, e64554 (2013). doi: 10.1371/journal.pone.0064554.
53. Cui, C. *et al.*, A novel two-component system modulates quorum sensing and pathogenicity in *Burkholderia cenocepacia*. *Mol. Microbiol.* **108**, 32-44 (2018). doi: 10.1111/mmi.13915.
54. Yang, C. *et al.*, *Burkholderia cenocepacia* integrates *cis*-2-dodecenoic acid and cyclic dimeric guanosine monophosphate signals to control virulence. *Proc. Natl Acad. Sci. U.S.A.* **114**, 13006-13011 (2017). doi: 10.1073/pnas.1709048114.
55. Guo, Q. *et al.*, Elongation factor P modulates *Acinetobacter baumannii* physiology and virulence as a cyclic dimeric guanosine monophosphate effector. *Proc. Natl Acad. Sci. U.S.A.* **119**, e2209838119 (2022). doi: 10.1073/pnas.2209838119.
56. Kang, Y., Zarzycki-Siek, J., Walton, C.B., Norris, M.H. & Hoang, T.T. Multiple FadD acyl-CoA synthetases contribute to differential fatty acid degradation and virulence in *Pseudomonas aeruginosa*. *PLoS One* **5**, e13557 (2010). doi: 10.1371/journal.pone.0013557.

57. Cui, B. *et al.*, The cell-cell communication signal indole controls the physiology and interspecies communication of *Acinetobacter baumannii*. *Microbiol. Spectr.* **10**, e0102722 (2022). doi: 10.1128/spectrum.01027-22.
58. Song, S. *et al.*, Anthranilic acid from *Ralstonia solanacearum* plays dual roles in intraspecies signalling and inter-kingdom communication. *ISME J.* **14**, 2248-2260 (2020). doi: 10.1038/s41396-020-0682-7.
59. Langmead, B. & Salzberg, S.L. Fast gapped-read alignment with Bowtie 2. *Nat. Methods* **9**, 357-359 (2012). doi: 10.1038/nmeth.1923.
60. Trapnell, C. *et al.*, Transcript assembly and quantification by RNA-Seq reveals unannotated transcripts and isoform switching during cell differentiation. *Nat. Biotechnol.* **28**, 511-515 (2010). doi: 10.1038/nbt.1621.
61. Song, S. *et al.*, An anthranilic acid-responsive transcriptional regulator controls the physiology and pathogenicity of *Ralstonia solanacearum*. *PLoS Pathog.* **18**, e1010562 (2022). doi: 10.1371/journal.ppat.1010562.
62. Landt, S.G. *et al.*, ChIP-seq guidelines and practices of the ENCODE and modENCODE consortia. *Genome Res.* **22**, 1813-1831 (2012). doi: 10.1101/gr.136184.111.
63. Kleinman, C.L., Sycz, G., Bonomi, H.R., Rodríguez, R.M., Zorreguieta, A. & Sieira, R. ChIP-seq analysis of the LuxR-type regulator VjbR reveals novel insights into the *Brucella* virulence gene expression network. *Nucleic Acids Res.* **45**, 5757-5769 (2017). doi: 10.1093/nar/gkx165.
64. Molecular Operating Environment (MOE), Chemical Computing Group Inc., 1010 Sherbooke St. West, Suite #910, Montreal, QC, Canada, H3A 2R7 (2018).
65. Yan, Y., Tao, H., He, J. & Huang, S.Y. The HDOCK server for integrated protein-protein docking. *Nat. Protoc.* **15**, 1829-1852 (2020). doi: 10.1038/s41596-020-0312-x.
66. Jumper, J. *et al.*, Highly accurate protein structure prediction with AlphaFold. *Nature* **596**, 583-589 (2021). doi: 10.1038/s41586-021-03819-2.

Acknowledgments

This work was financially supported by the National Key Research and Development Program of China (2021YFA0717003 to Y.D.), the National Natural Science Foundation of China (32300033 to S.S.) and the Scientific Research Foundation of Hainan University (KYQD(ZR)-23006 to S.S.).

Author contributions

Y.D. and S.S. conceived the project. S.S., X.L., J.L., and Y.D. designed the research. S.S., X.L., J.L., B.W., Y.S., H.H., X.S., M.W., and B.C. performed the research. S.S., X.L., J.L., G.W., Y.H., L.X., B.G., L.Y., X.W., L-H.Z., and Y.D. analyzed the data. S.S. and Y.D. wrote the paper.

Competing interests

The authors declare no competing interests.

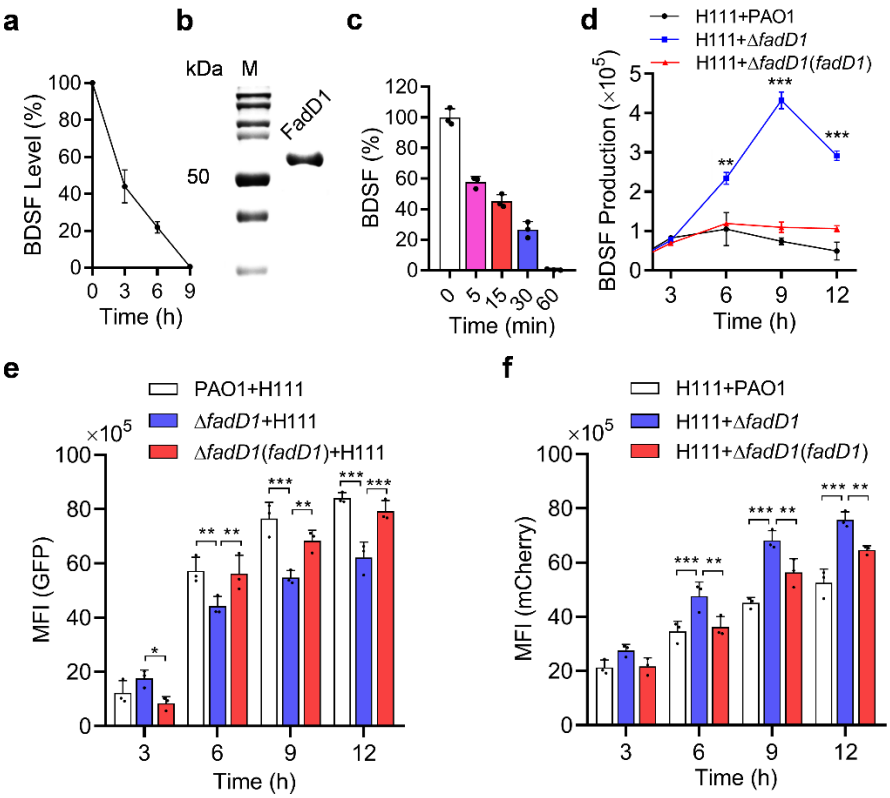

Figure 1. Effect of *fadD1* on the competitive capability of *P. aeruginosa* against *B. cenocepacia*. **a** Analysis of the BDSF signal quenching ability of *P. aeruginosa* PAO1 (n = 3 biological replicates). **b** SDS-PAGE of the purified FadD1 protein. **c** Analysis of the enzymatic quenching activity of FadD1 on BDSF signal (*n* = 3 biological replicates). **d** The BDSF signal production of the *B. cenocepacia* H111 strain cocultured with *P. aeruginosa* PAO1 wild-type, Δ*fadD1* and Δ*fadD1*(*fadD1*) strains (*n* = 3 biological replicates). ***p*=0.0016, ****p*<0.001, ****p*<0.001. **e** Green mean fluorescence intensity of the *P. aeruginosa* PAO1 wild-type, Δ*fadD1* and Δ*fadD1*(*fadD1*) strains carrying the green fluorescent protein expression vector (*n* = 3 biological replicates). **p*=0.0306, ***p*=0.0021, ***p*=0.0050, ****p*<0.001, ***p*=0.0017, ****p*<0.001, ****p*<0.001. **f** Red mean fluorescence intensity of the *B. cenocepacia* H111 strain carrying the mCherry fluorescent protein expression vector (*n* = 3 biological replicates). ****p*<0.001, ***p*=0.0016, ****p*<0.001, ***p*=0.0011, ****p*<0.001, ***p*=0.0020. The data are the means ± standard deviations of three independent experiments. The *P. aeruginosa* PAO1 wild-type, Δ*fadD1* and Δ*fadD1*(*fadD1*) strains carried the green fluorescent protein expression vector. The mCherry fluorescent protein expression vector was carried by the *B. cenocepacia* H111 strain. The *P. aeruginosa* PAO1 wild-type, Δ*fadD1* and Δ*fadD1*(*fadD1*) strains were cocultured with *the B. cenocepacia* H111 strain at a ratio of 1:4 (v/v) at OD_{600} = 0.1. The statistical comparisons were

performed using two-way ANOVA. In **b** experiment was performed three times and representative images from one experiment are shown.

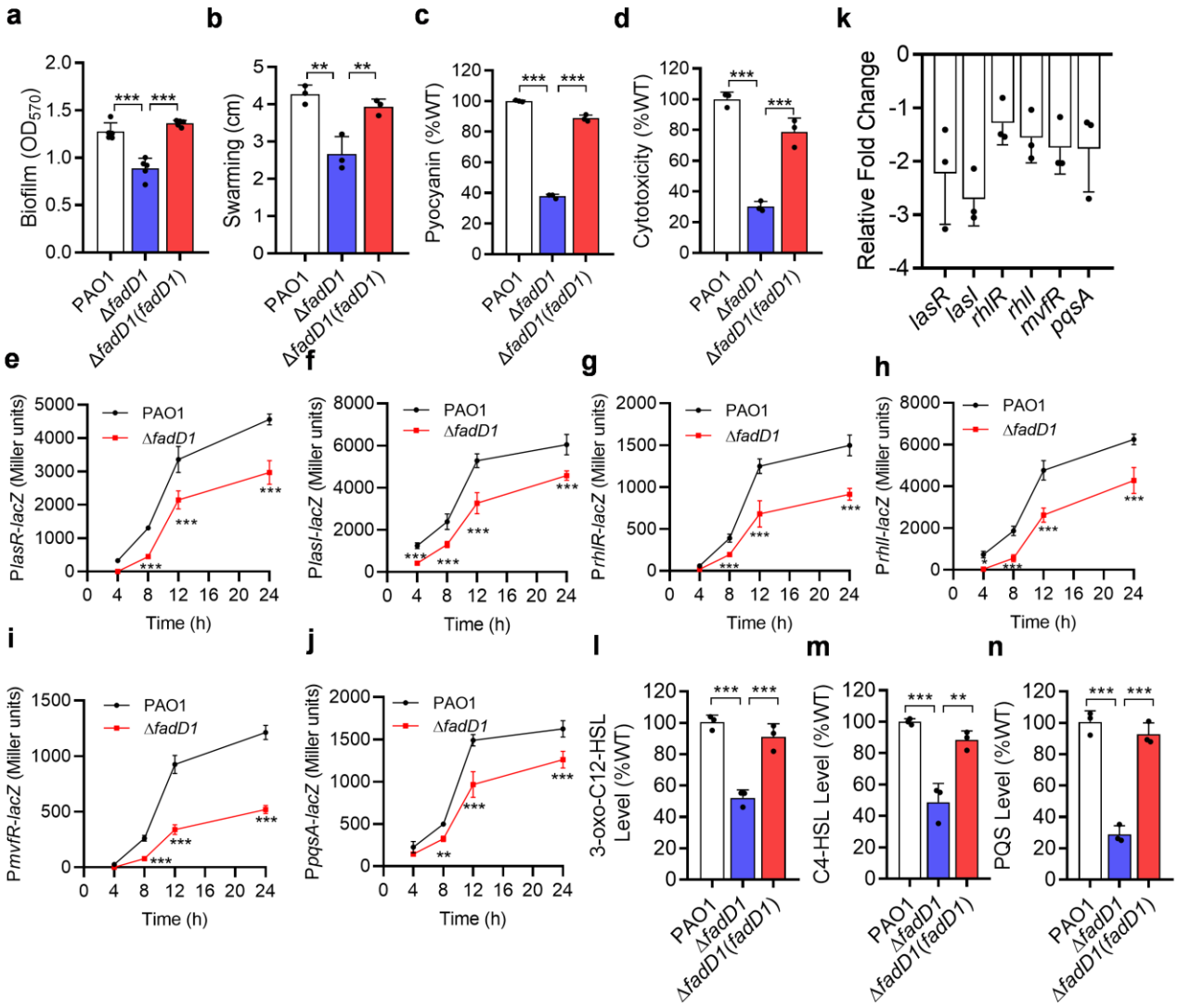

Figure 2. Effects of *fadD1* on the QS-regulated phenotypes and QS of *P. aeruginosa*. Analysis of biofilm formation **a**, swarming motility **b**, pyocyanin production **c**, and virulence **d** in *P. aeruginosa* PAO1(**a**, *n* = 5 biological replicates; **b**, **c**, **d**, *n* = 3 biological replicates). **a** ***p<0.001, ***p<0.001. **b** **p=0.0025, **p=0.0081. **c** ***p<0.001, ***p<0.001. **d** ***p<0.001, ***p<0.001. Effects of *fadD1* on the gene expression levels of *lasR* **e**, *lasI* **f**, *rhlR* **g**, *rhlI* **h**, *mvfR* **i** and *pqsA* **j** by assessing the β-galactosidase activity of the promoter-*lacZ* transcriptional fusions and by RT-qPCR **k**, which are the signal molecule synthase-encoding genes and receptor genes of the *rhl*, *las* and *pqs* QS systems in *P. aeruginosa* PAO1, respectively (*n* = 3 biological replicates). **e** ***p<0.001, ***p<0.001, ***p<0.001. **f** ***p<0.001, ***p<0.001, ***p<0.001, ***p<0.001. **g** ***p<0.001, ***p<0.001, ***p<0.001. **h** *p=0.025, ***p<0.001, ***p<0.001, ***p<0.001. **i** ***p<0.001, ***p<0.001, ***p<0.001. **j** **p=0.0015, ***p<0.001, ***p<0.001. The production of 3-oxo-C12-HSL **l**, C4-HSL **m** and PQS **n** in the *P. aeruginosa* PAO1 wild-type, Δ*fadD1* and Δ*fadD1*(*fadD1*) strains (*n* = 3 biological replicates). The production of QS

signals in the *P. aeruginosa* PAO1 wild-type strain was arbitrarily defined as 100%. **l** ***p<0.001, ***p<0.001. **m** ***p<0.001, **p=0.0015. **n** ***p<0.001, ***p<0.001. The data are means ± standard deviations of three independent experiments. The statistical comparisons were performed using one-way ANOVA or two-way ANOVA (**a**, **b**, **c**, **d**, **l**, **m**, **n**, one-way ANOVA; **e**, **f**, **g**, **h**, **i**, **j**, two-way ANOVA).

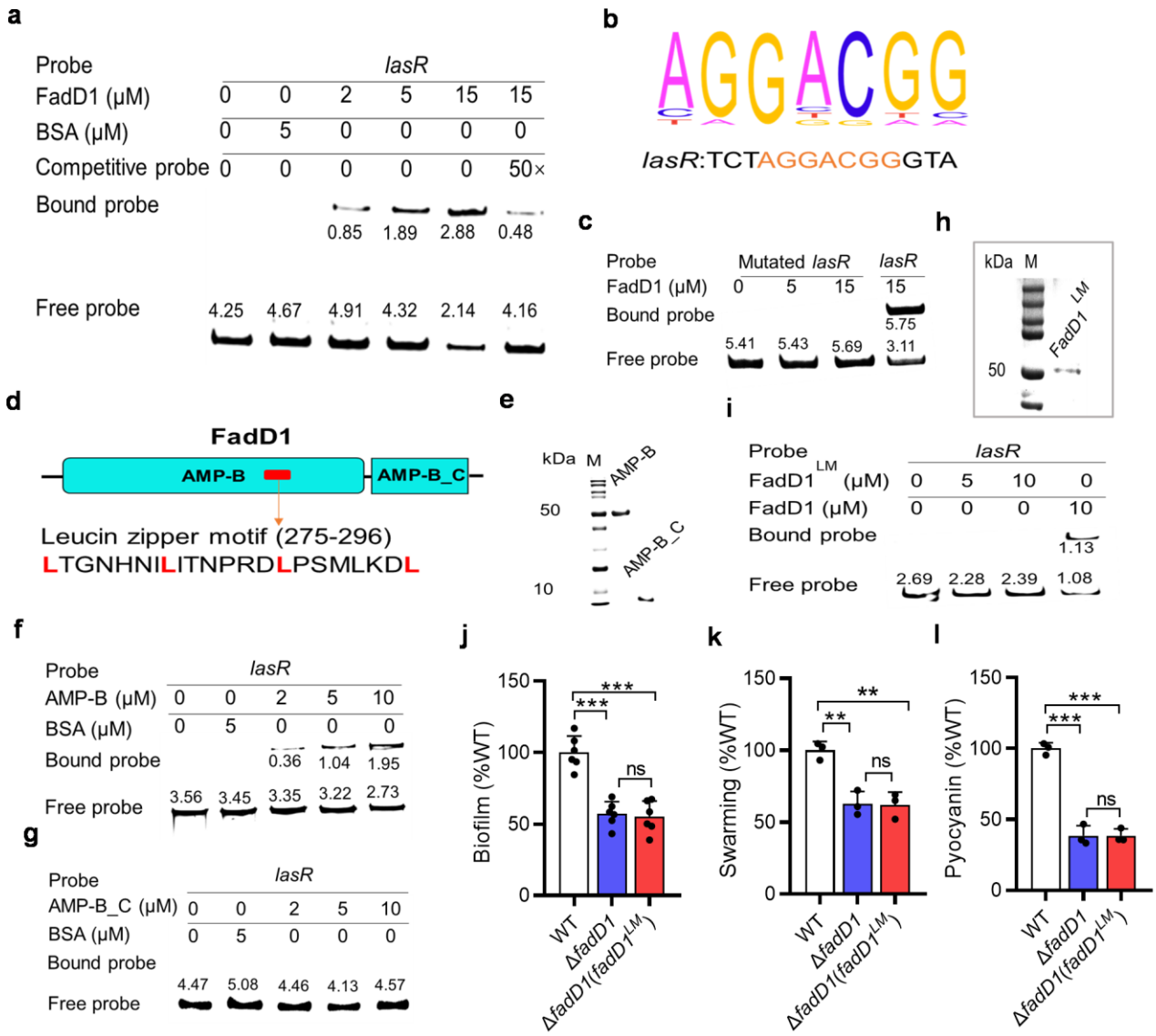

Figure 3. Analysis of the binding of FadD1 to target gene promoters. a EMSA analysis of *in vitro* binding of FadD1 to the promoter of *lasR*, in which the biotin-labeled 339-bp *lasR* promoter DNA probe was used for the protein binding assay. A protein-DNA complex, represented by a band shift, was formed when different concentrations of FadD1 protein were incubated with the probe at room temperature for 30 min. **b** A potential FadD1 binding region was identified by ChIP-seq. The conserved sequence is shown in orange. **c** Analysis of the binding between FadD1 and the mutated *lasR* promoter with deletion of the FadD1 binding sequence AGGACGG. EMSA analysis was performed *in vitro*. **d** Domain structure analysis of FadD1 (https://www.ebi.ac.uk/Tools/hmmer/). The red box represents the leucine zipper motif (https://www.novopro.cn/tools/motifscan.html) in AMP-B domain. **e** SDS-PAGE of the purified AMP-B domain and the AMP-B_C domain of the FadD1 protein.

EMSA analysis of *in vitro* binding of the AMP-B domain **f** and the AMP-B_C domain **g** to the promoter of *lasR*. **h** SDS-PAGE of the purified mutated FadD1 protein ($FadD1^{LM}$: L275A L282A L289A L296A). **i** EMSA analysis of the *in vitro* binding of the mutated FadD1 protein to the promoter of *lasR*. *In trans* expression of the mutated *fadD1* could not restore biofilm formation **j**, swarming motility **k**, and pyocyanin production **l** in the *P. aeruginosa* Δ*fadD1* strain (**j**, n = 6 biological replicates; **k**, **l**, n = 3 biological replicates). **j** ***p<0.001, ***p<0.001, ^{ns}p=0.9362. **k** **p=0.0029, **p=0.0026, ^{ns}p=0.9919. **l** ***p<0.001, ***p<0.001, ^{ns}p>0.9999. The EMSA experiments were performed three times, and representative images from one experiment are shown. The data are the means ± standard deviations of three independent experiments. The statistical comparisons were performed using one-way ANOVA.

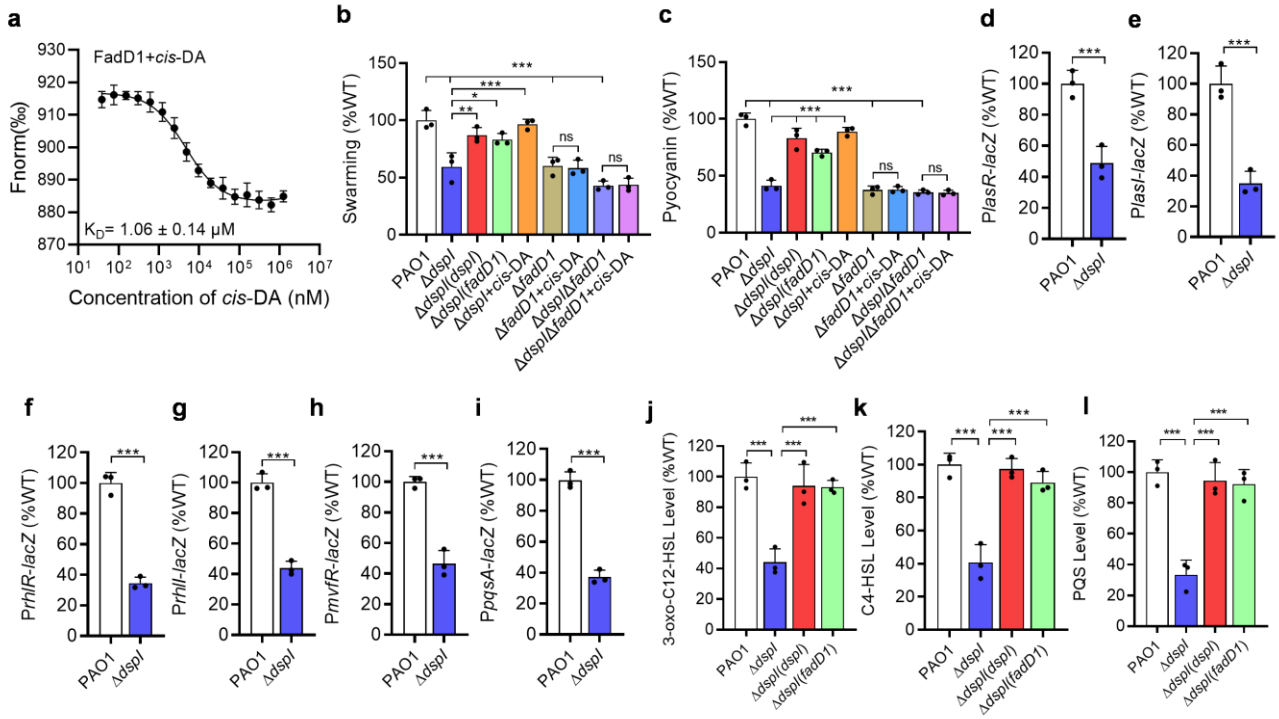

Figure 4. Effects of FadD1 on *cis*-DA-regulated phenotypes of *P. aeruginosa*. a MST analysis of the binding of *cis*-DA to the FadD1. "Fnorm (‰)" indicates the fluorescence time trace changes in the MST response. Complementation of the *dspI* mutant with *fadD1*. *In trans* expression of *fadD1* complemented swarming motility **b** and pyocyanin production **c** in the *dspI*-deficient mutant. Effects of *dspI* on the gene expression levels of *lasR* **d**, *lasI* **e**, *rhlR* **f**, *rhlI* **g**, *mvfR* **h**, *pqsA* **i** and the production of 3-oxo-C12-HSL **j**, C4-HSL **k** and PQS **l** of the *P. aeruginosa* PAO1 strains. The production of QS signals in the *P. aeruginosa* PAO1 wild-type strain was arbitrarily defined as 100%. n = 3 biological replicates. **b** ***p<0.001, ***p<0.001, *p=0.0181, **p=0.0047, ^{ns}p>0.9999, ^{ns}p>0.9999. **c** ***p<0.001, ***p<0.001, ^{ns}p=0.9984, ^{ns}p>0.9999. **d**, **e**, **f**, **g**, **h**, **l**, **j**, **k**, **l** ***p<0.001. The data are means ± standard deviations of three independent experiments. The statistical comparisons were performed using one-way ANOVA.

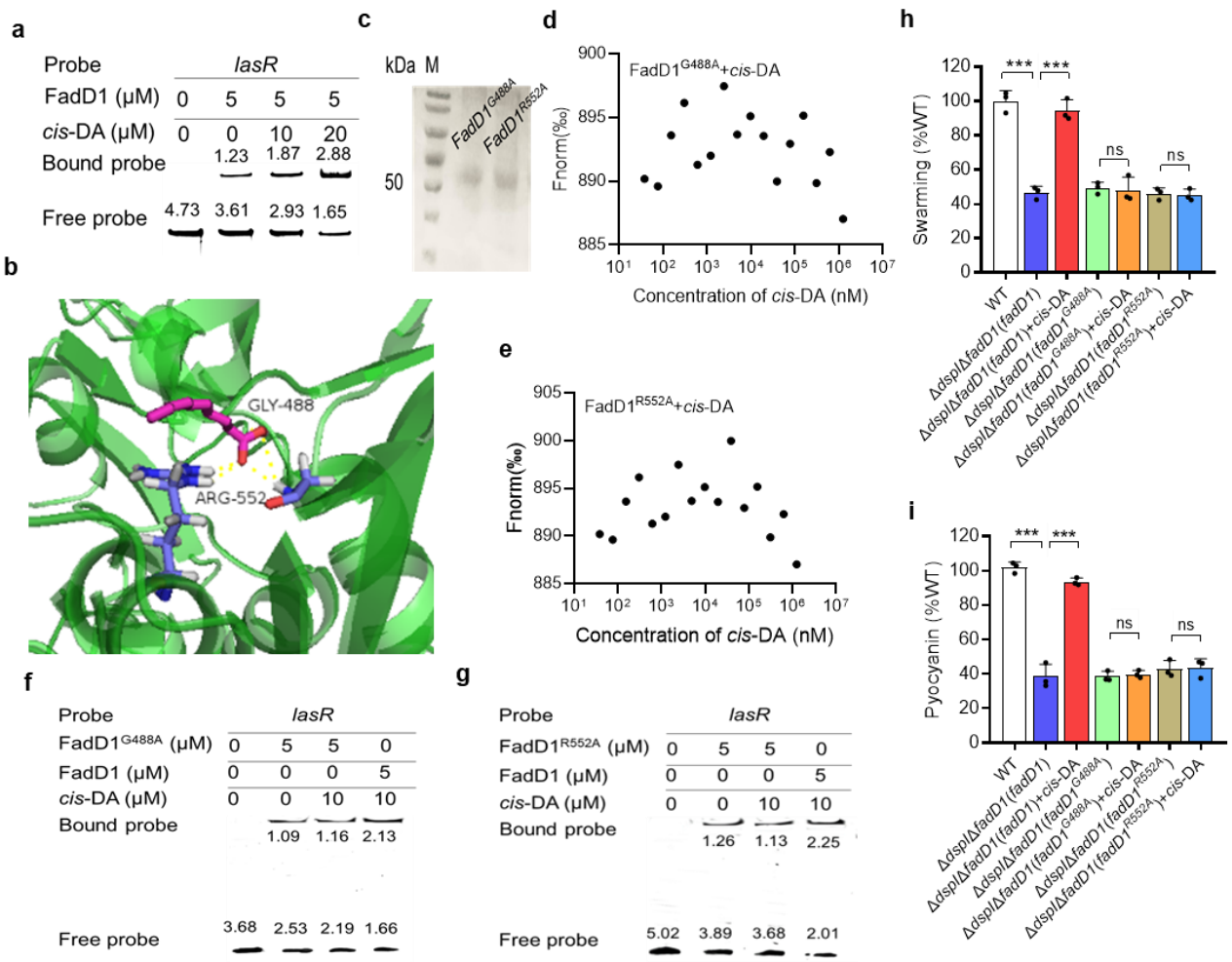

Figure 5. Effects of *cis*-DA on the binding of FadD1 to the promoters of the target genes. a EMSA analysis of the *in vitro* binding of FadD1 to the promoter of *lasR* with the addition of different amounts of *cis*-DA. **b** The potential residues (which are shown as stick models and are labeled) of FadD1 involved in *cis*-DA binding analyzed by AutoDocking software. The hydrogen bonds were represented by yellow dashed lines. **c** SDS–PAGE gel electrophoresis of purified FadD1 variants. MST analysis of the binding of BDSF to the **d** FadD1^{G488A} and **e** FadD1^{R552A}. EMSA analysis of the *in vitro* binding of **f** FadD1^{G488A} and **g** FadD1^{R552A} to the promoters of *lasR* with the addition of different amounts of *cis*-DA. The EMSA experiments were performed three times, and representative images from one experiment are shown. Analysis of the perception of *cis*-DA by FadD1^{G488A} and FadD1^{R552A}, *cis*-DA-regulated phenotypes: **h** swarming motility and **i** pyocyanin production in *P. aeruginosa* (n = 3 biological replicates). **h** ***p<0.001, ***p<0.001, ^{ns}p>0.9999, ^{ns}p>0.9999. **i** ***p<0.001, ***p<0.001, ^{ns}p=0.9996, ^{ns}p>0.9999. The data are means ± standard deviations of three independent experiments. The statistical comparisons were performed using one-way ANOVA.

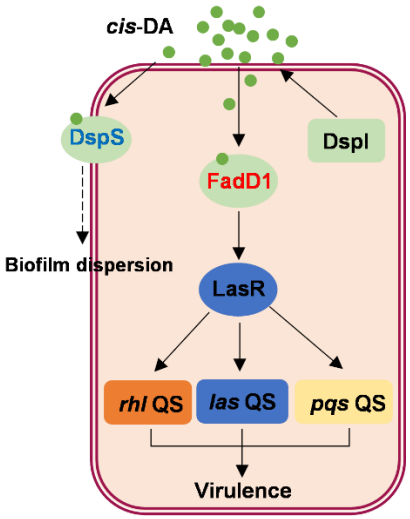

Figure 6. Schematic representation of *cis*-DA-regulated QS signaling in *P. aeruginosa*. DspI synthesized *cis*-DA signal molecule. FadD1, the signal receptor of *cis*-DA, perceives *cis*-DA signal and regulates the transcription of *lasR*, which positively regulates the *las*, *rhl* and *pqs* QS systems in *P. aeruginosa*. DspS is also the sensor of *cis*-DA involved in biofilm dispersion in response to *cis*-DA. The individual QS circuits are highly interconnected.